ETHIOPIAN JOURNAL OF TEXTILE AND APPAREL
EJTEX
ETHIOPIAN INSTITUE OF TEXTILE AND FASHION TECHNOLOGY BAHIR DAR UNIVERSITY, ETHIOPIA

EXPERIMENTAL EVALUATION OF THERMAL AND MECHANICAL PERFORMANCES OF PLASTICIZED SISAL FIBER–REINFORCED POLYLACTIC ACID COMPOSITES UNDER VARIABLE CONDITIONS

Eshetie Kassegn[1], Mehari B. Teshome[2]

[1]Faculty of Mechanical and Industrial Engineering, 231 Mekelle University, Ethiopia.

[2]Department of Mechanical Engineering, AASTU, Addis Ababa, Ethiopia.

ISSN: (Print) (Online) Journal homepage: https://journals.bdu.edu.et/index.php/ejta

To cite this article: Eshetie Kassegn et al. (2026), EXPERIMENTAL EVALUATION OF THERMAL AND MECHANICAL PERFORMANCES OF PLASTICIZED SISAL FIBER–REINFORCED POLYLACTIC ACID COMPOSITES UNDER VARIABLE CONDITIONS, 46-61

EXPERIMENTAL EVALUATION OF THERMAL AND MECHANICAL PERFORMANCES OF PLASTICIZED SISAL FIBER–REINFORCED POLYLACTIC ACID COMPOSITES UNDER VARIABLE CONDITIONS

Eshetie Kassegn[1*], Mehari B. Teshome[2]

[1]Bahir Dar Energy Center, Bahir Dar Technology Institute, Bahir Dar University, Bahir Dar,

[2]Ethiopian Institute of Textile and Fashion Technology, Bahir Dar University, Po.Box 1037, Bahir Dar, Ethiopia

[*]Corresponding Author:

Email: eshetie.kassegn@mu.edu.et

ABSTRACT

Recently, the focus of global researchers is on the development and characterization of natural fiber-reinforced bio-based polymer composites for various engineering applications. In this study, composites of PLA and sisal fiber were fabricated using injection molding, with acetyl tributyl citrate added as a plasticizer. Composites were characterized through mechanical, thermal and rheological analyses to assess the effects of the fiber content and the plasticizer on the mechanical, thermal and rheological properties of the composites. In addition, differential scanning calorimetry test results indicated that PLA crystallinity increased with the addition of both fiber and plasticizer, although the contribution of fiber alone was relatively limited. The inclusion of the plasticizer also led to a reduction in the glass transition temperature of PLA. Thermal property analysis further revealed that fiber content and processing temperature had a significant influence on thermal conductivity of composites. Thermal conductivity increased with rising fiber content and temperature up to 50°C but decreased at temperatures above this threshold. Dynamic mechanical analysis showed that the storage and loss moduli of the composites were temperature-dependent. The storage modulus increased with fiber content but declined sharply near the glass transition temperature. Rheological characterization demonstrated effective fiber–fiber and fiber–matrix interactions, resulting in good fiber dispersion within the PLA matrix. This contributed to stable shear viscosity across a wide range of shear rates for different capillary dimensions. Viscosity increased with higher fiber content but decreased with plasticizer addition. Temperature also played a critical role, as viscosity decreased with increasing melt temperature.

Keywords: Composite; mechanical properties; PLA; sisal fiber; thermal behavior.

INTRODUCTION

The development of high-strength, low-cost polymer composites has been a central focus of research for many years. The growing adoption of polymer composites has become increasingly important across a wide range of industrial and household applications (Mann *et al.*, 2020). The use of polymeric composites is growing due to their interesting properties over other engineering materials (Kassegn *et al.*, 2021). This expansion is largely driven by their superior properties compared to conventional materials.

More recently, significant attention has shifted toward environmentally friendly composites made from biodegradable polymers and natural fibers. These materials are gaining popularity due to their potential for biodegradability, suitability for diverse industrial applications, satisfactory mechanical performance, and relatively simple manufacturing processes (Morales *et al.*, 2017). As a result, such composites are increasingly replacing components traditionally made from synthetic fiber–reinforced materials in the automotive sector, including door panels, trunk panels, and headliners (Choudhury and Debnath, 2019). However, mechanical and thermal properties of natural fiber-reinforced polymer composites under variable conditions are not well-studied.

Therefore, the aim of this study is to investigate the mechanical and thermal performances of sisal-PLA composites with/without the addition of plasticizer.

Studying natural fiber reinforced polymer composites under variable conditions is vital for determining their applicability. Moreover, effects of temperature and moisture on mechanical and thermal properties of composites are important to be determined before intending the composite for outdoor application.

2. LITERATURE REVIEW

Some previous studies highlight the importance of investigating the effects of environmental challenges, particularly temperature and moisture absorption on the mechanical and thermal performance of bio-based composite materials.

2.1. Environmental Challenges

In response to environmental challenges, bio-based polymer materials are receiving more and more attention. Polylactic acid (PLA) is one of the bio-based and biodegradable polymers made from natural sources such as corn and starch (Saeed, Nawaz and Al-Turaif, 2018), and has emerged as a promising thermoplastic material for eco-friendly composites, due to its interesting mechanical properties and biodegradability (Qi, Ren and Wang, 2017),(Elsawy *et al.*, 2017). PLA matrix and its composites have been widely used for food packaging, biomedicine and fiber textile applications (Ortenzi *et al.*, 2020),(Jing *et al.*, 2021). This is mainly attributed to the biodegradability and non-toxicity properties of PLA. Additionally, natural fibers are a potential reinforcement. This is due to their interesting properties such as high mechanical properties, low cost, low weight, high specific strength and modulus, environmentally friendly and biodegradability characteristics (Sanjay and Yogesha, 2018). Among natural fibers, sisal fibers (SFs) have the potential to replace synthetic fibers and other natural fibers. This is due to its excellent mechanical properties (Table 1) and abundant availability (Veerasimman *et al.*, 2022). The mechanical properties of composites are effected by the weight fraction of reinforcement and fiber-matrix adhesion (Delgado-Aguilar *et al.*, 2017).

2.2. Mechanical Properties of Biocomposites

According to previous studies, natural fiber reinforced polymer composite materials have been reported to exhibit comparable mechanical properties to the synthetic fiber reinforced composites (Sanjay *et al.*, 2018),(Sanjay *et al.*, 2018). Despite this, the adhesion between natural fibers and polymer matrix (especially hydrophobic polymers) is poor (Jing *et al.*, 2021), which affects composite performance. Additionally, there are some shortcomings of natural fibers as a reinforcement in composites such as poor interface adhesion, maximum processing temperature limited to 200oC and low dimensional stability (Morales *et al.*, 2017). In order to find solutions to these issues, researchers have been conducting a great deal of experimental research. Composite properties such as tensile strength, flexural strength and impact strength are all related to the fiber-matrix adhesion strength (Sanjay and Yogesha, 2018).

2.3. Thermal Properties of Biocomposites

The study of the thermal characteristics of natural fiber reinforced polymer composites has been gaining attention to understand their behaviour at elevated processing temperatures (Cristina *et al.*, 2020). Recent research has focused on the thermal properties of bio-based polymers. Bio-based polymers have a limited processing temperature, since their thermal degradation starts at temperatures just above their melting point (Cataldi *et al.*, 2020). Moreover, Natural fiber reinforcements affect the thermal stability, crystallization, and melting behaviour of biocomposite materials (Akderya, Özmen and Baba, 2020). The thermal stability of biopolymer composites increases because of the presence of reinforcements. Additionally, rheological properties

of polymer composites are studied to evaluate their processing behaviour (Zhang *et al.*, 2020). It has been reported in previous studies that reinforcement affects the rheological properties of PLA composites (Snowdon *et al.*, 2019).

2.4. Impact of Plasticizers in Biocomposites

Improving the impact resistance of composites is crucial for applications requiring high energy absorption. Plasticizers have been investigated for their impact-modifying capabilities in composites. Eshetie et al. (Kassegn *et al.*, 2023) and Selvaraj et al. (Selvaraj *et al.*, 2019) observed a significant increase in impact strength when specific plasticizers were added to sisal fiber-reinforced polylactic acid composites and natural fiber-reinforced polymer composites. These plasticizers enhanced the energy dissipation capacity of the composites, resulting in improved impact resistance. Khan et al. (Khan, 2019) found that the addition of plasticizers to sago starch-reinforced low-density polyethylene composites improved impact strength by enhancing matrix toughness, fiber-matrix compatibility, and chain mobility. Therefore, the incorporation of compatible plasticizers in composites can significantly enhance impact strength and damping resistance (Haque *et al.*, 2015; Gupta and Singh, 2018; Cheour *et al.*, 2020; Liu *et al.*, 2021).

Table 1 The mechanical properties of natural fibers.

Fiber type	Density [g/cm^3]	Elastic modulus [GPa]	Tensile strength [MPa]	Strain at failure [%]	Reference
Sisal	1.33	38	650	2.5	(Veerasimman *et al.*, 2022)
Bamboo	1.36	52	658	1.3	(Depuydt *et al.*, 2017)
Flax	1.45	60	710	-	(Ali *et al.*, 2018)
Enset	1.52	22	155	2.1	(Bekele, Lemu and Jiru, 2022)
Jute	1.45	14	393	-	(Dwivedi, Pattnaik and Kumar Sutar, 2021)
Hemp	1.47	44	584	1.6	(Murariu and Dubois, 2016)
Banana	1.35	8	644	2.3	(Sanjay *et al.*, 2018)
Kenaf	1.20	53	743	1.6	(Lalit, Mayank and Ankur, 2018)

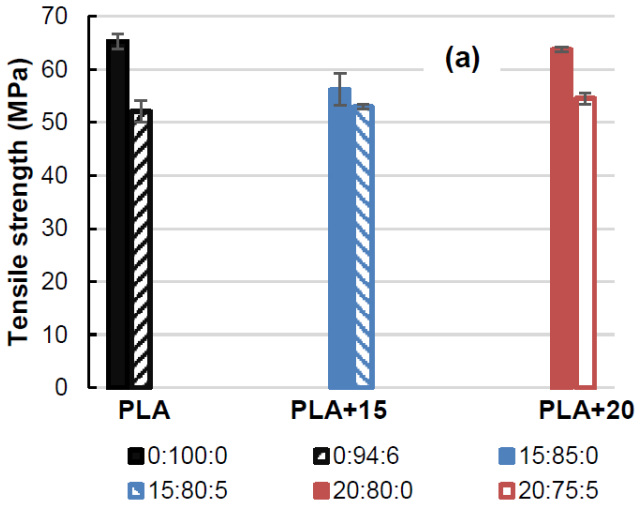

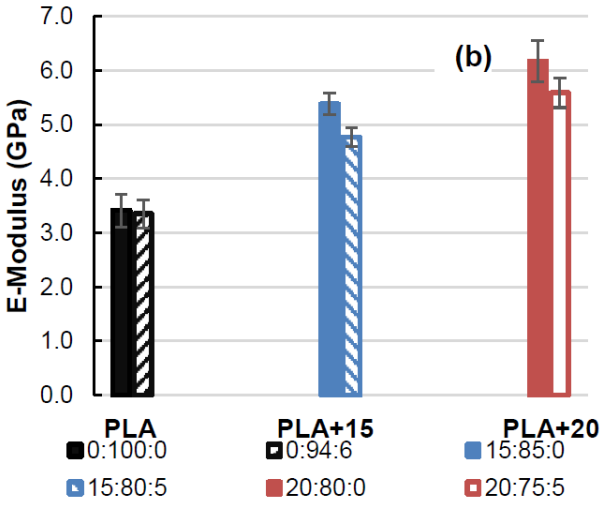

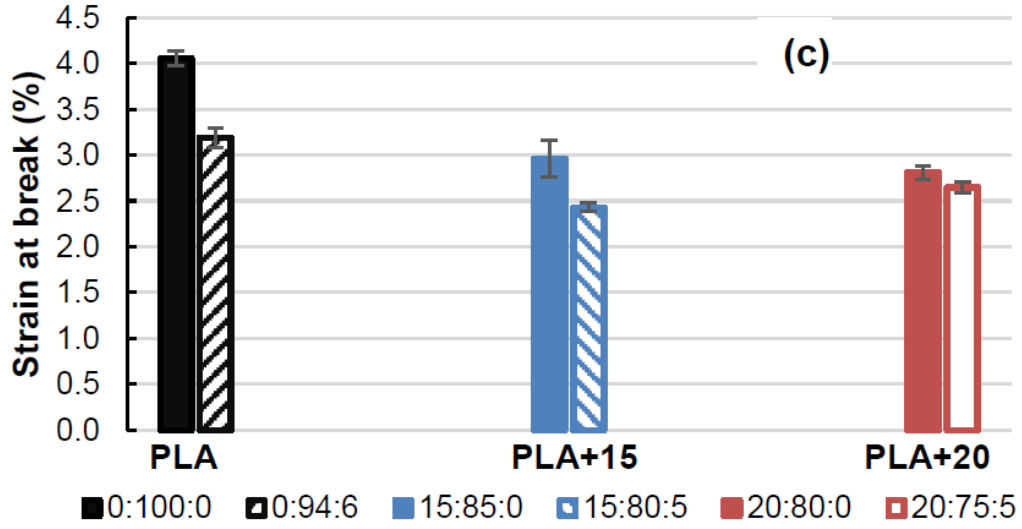

Figure 1 The tensile strength (a), tensile modulus (b), and tensile strain at break (c) of SF-PLA composites.

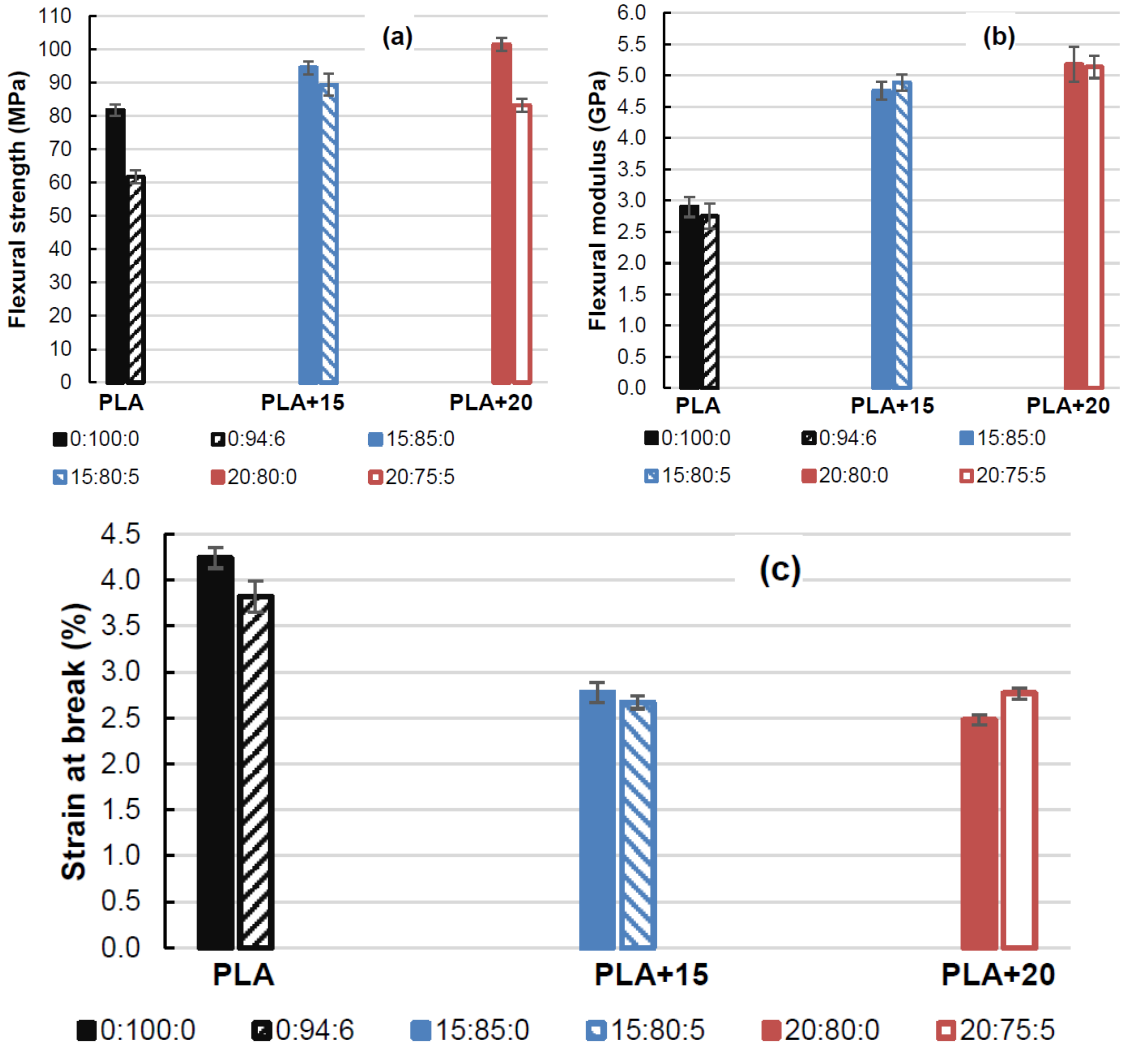

Figure 2 The flexural strength (a), flexural modulus (b), and flexural strain at break (c) of SF-PLA composites.

Figure 3. The impact strength of SF-PLA composites.

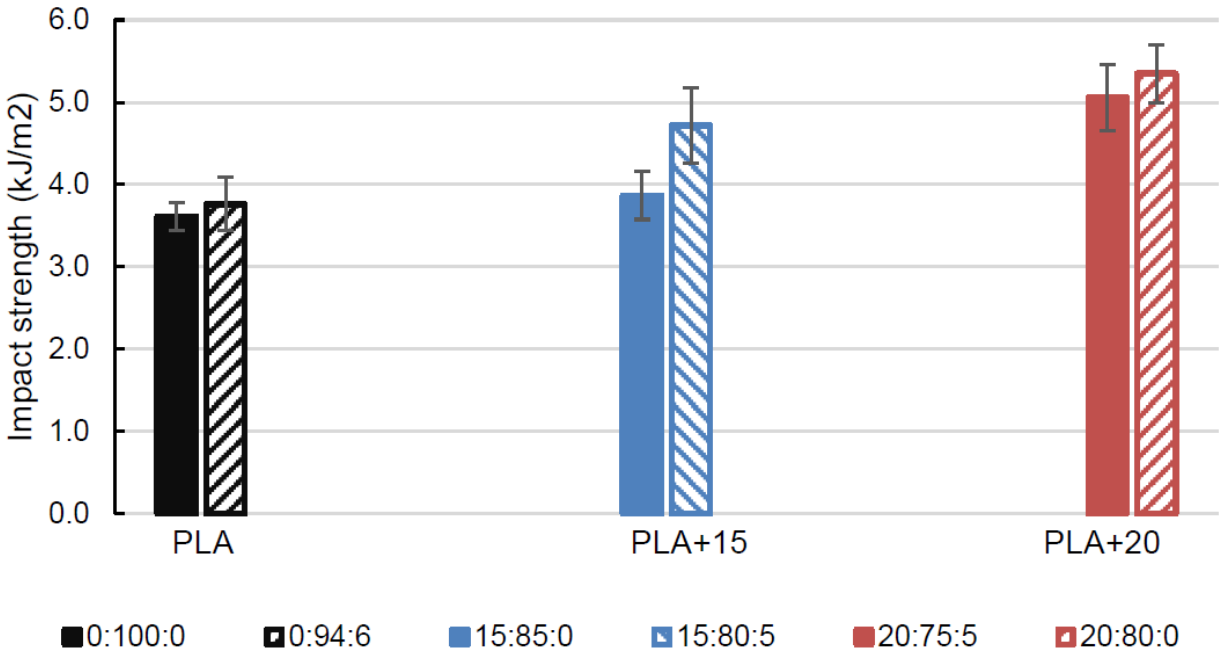

Figure 3 The impact strength of SF-PLA composites.

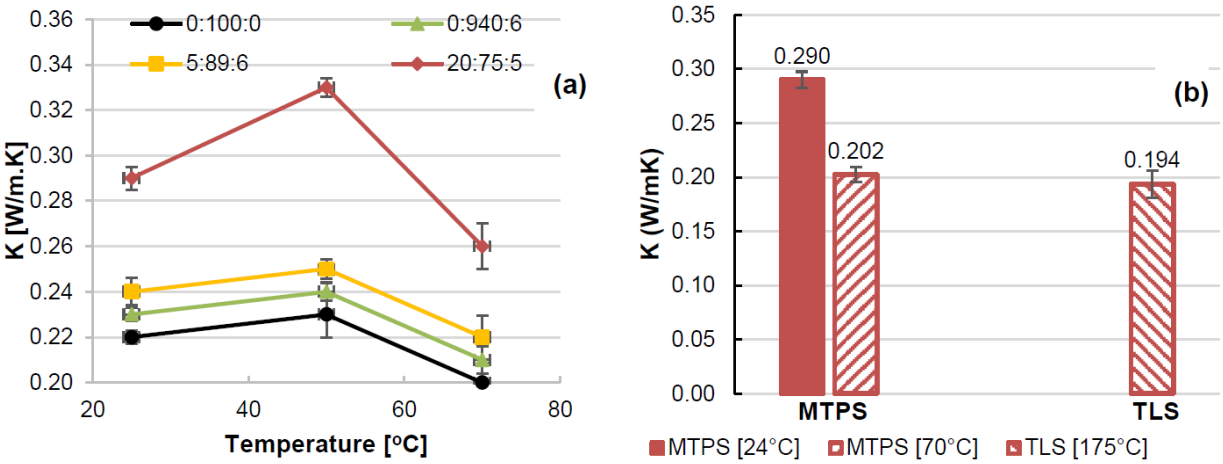

Figure 4 Thermal conductivity with MTPS (a) and thermal conductivity of 20:75:5 with MTPS and TLS (b).

Table 2 DSC testing results of SF-PLA composites.

SF:PLA:ATBC [wt%]	T_g [°C]	T_{cc} [°C]	T_m [°C]	ΔH_{cc} [J/g]	ΔH_m [J/g]	X_c [%]
0:100:0	63.5	145.9	152.6	7.9	11.1	3.5
0:94:6	52.6	138.3	145.9	19.6	25.1	6.2
5:89:6	51.9	137.7	145.3	20.3	23.5	3.9
15:80:5	53.4	138.3	146.1	15.2	19.1	5.4
20:80:0	63.8	143.8	150.0	15.0	17.6	3.6
20:75:5	55.1	138.8	148.1	15.1	19.8	6.9

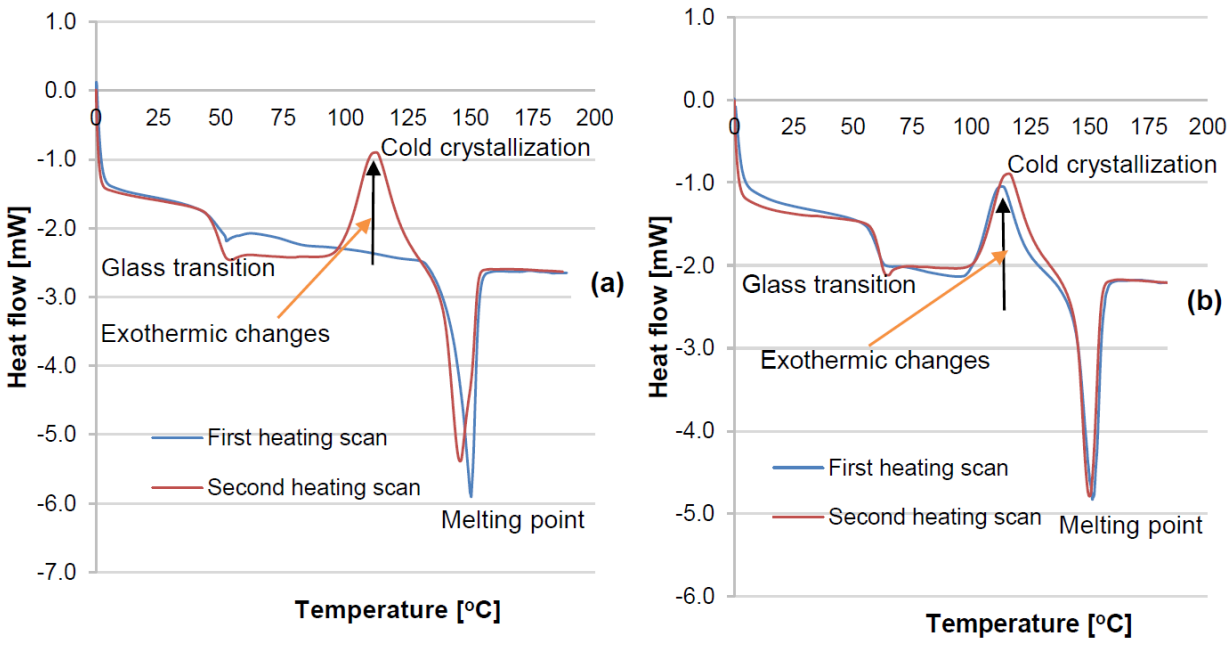

Figure 5 Cold crystallization behavior of PLA matrix with the addition of ATBC plasticizer (a), without incorporation of ATBC plasticizer (b).

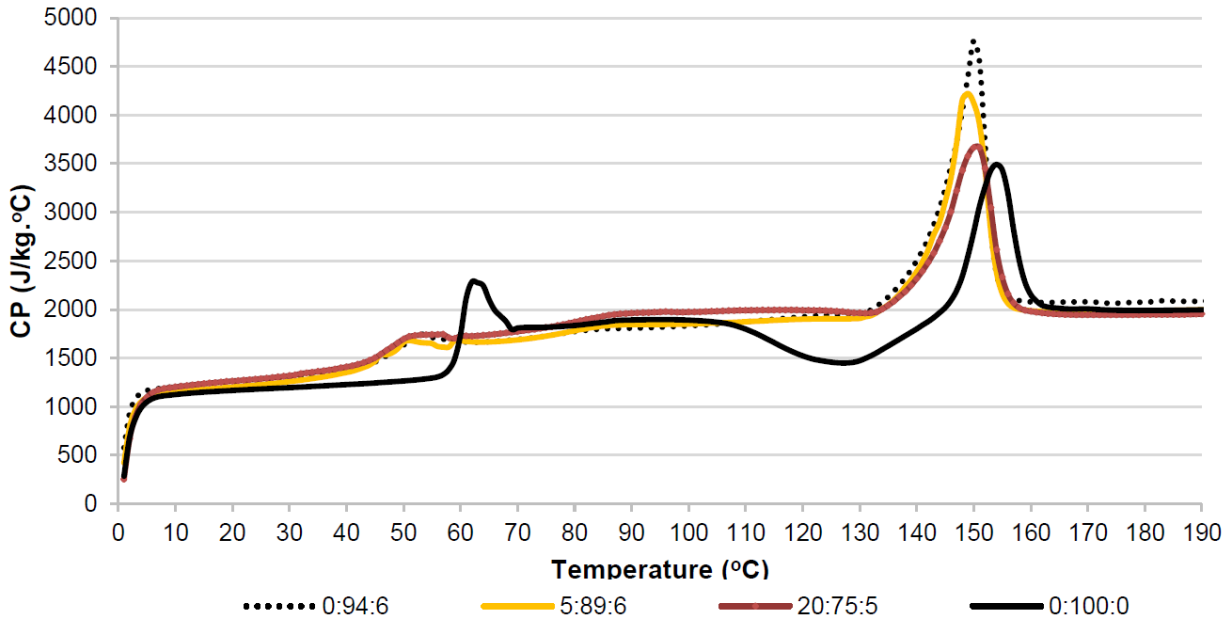

Figure 6 Specific heat capacity of SF-PLA composites as a function of temperature.

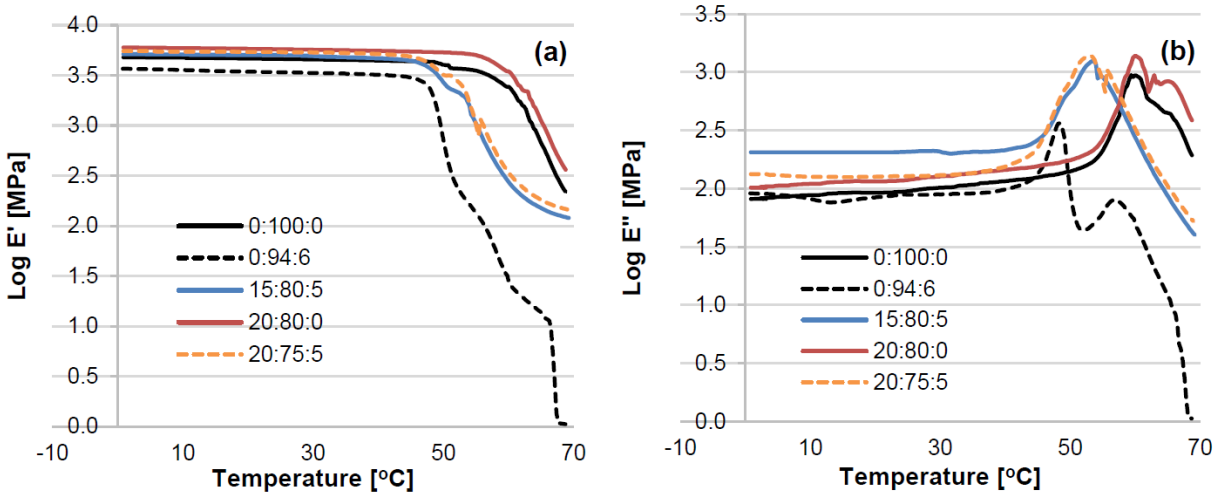

Figure 7 DMA measurements of SF-PLA composites for storage modulus (a) and loss modulus (b).

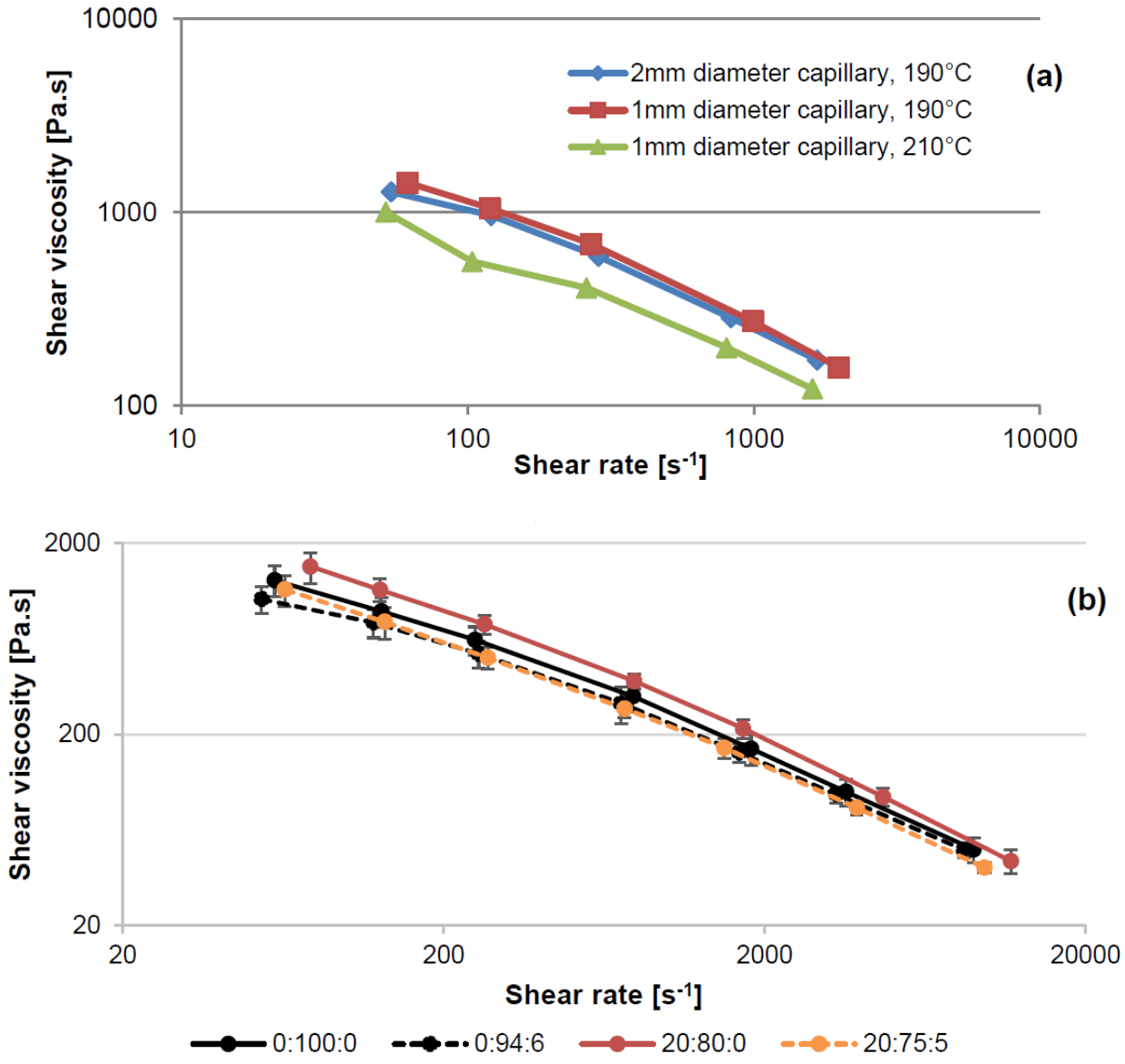

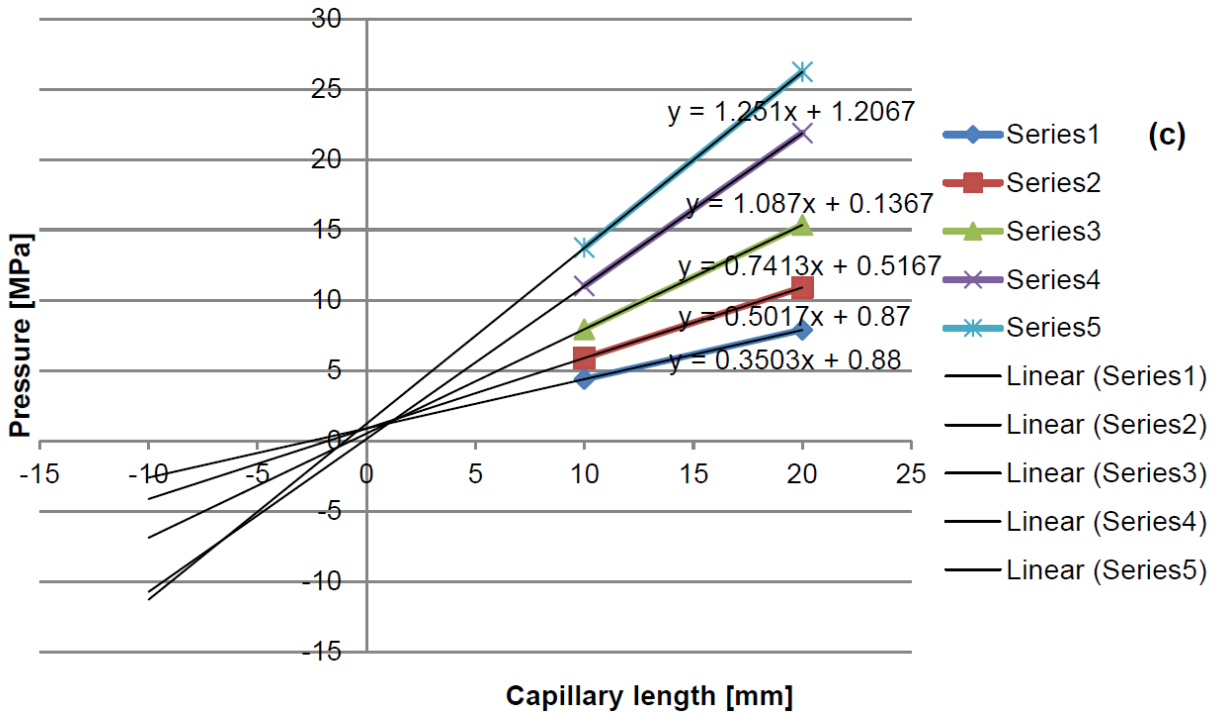

Figure 8 Shear viscosity of 20:75:5 composite (a), shear viscosity of composites with various fiber contents (b), and pressure required on capillary length of (c) using RheoArt rheometer.

3. METHODOLOGY

The reinforcement, matrix and plasticizer have been selected based on their biodegradability. Composites were processed using optimum process parameters. All data were collected from experimental testing.

3.1. Materials

Polylactic acid (PLA) with 95% L-lactic acid and 5% D-lactic acid and 110,000 g/mol molecular weight (Backes *et al.*, 2019) was used. Sisal fiber (SF) were used as reinforcement in the composites. The fibers were collected from Abala of Afar region, Ethiopia. For the investigation of the mechanical and thermal properties of biocomposites, different weight percentages (wt%) of SF were applied. Before injection moulding, the fibers were cut to an approximate length of 5 mm. acetyl tributyl citrate (ATBC) plasticizer was used in the composites.

3.2. Composite Processing

PLA-based composites containing SF were processed through a twin screw extruder for melt-mixing, and injection moulding machine for specimen fabrication. Composites with fiber content ranging from 0 to 20% were prepared. The composite of SF:PLA:ATBC with wt% of 0:100:0, 0:94:6, 5:95:0,5:89:6, 15:85:0, 15:80:5, 20:80:0 and 20:75:5 were prepared. Melt-mixed pellets were used to perform TLS thermal conductivity and differential scanning calorimetry (DSC) tests. Injection-molded specimens were used to perform mechanical, dynamic mechanical analysis (DMA) as well as MTPS thermal conductivity tests.

3.3. Mechanical Tests

3.3.1 Tensile Testing

Tensile specimen fabrication and testing was performed according to ISO 527 standard (ISO, 2006). The tests were performed using an Instron 3367 testing machine with a load cell of 30 kN and a testing rate of 5 mm/min. An extensometer was used to measure the initial strain of the specimens. It was removed from samples at 1% strain. The tests were conducted at room temperature and relative humidity of 40%. The tests were conducted on five specimens of each material composition.

3.3.2 Flexural Testing

Three-point bending specimen preparation and testing was carried out according to ISO 178 standard (ISO, 2019). The tests were performed using an Instron 3367 testing machine with a load cell of 30 kN and a testing rate of 2 mm/min. The maximum displacement of the specimen was tuned to 10 mm. The tests were carried out at room temperature and relative humidity of 40%. Five specimens of each material composition were tested.

3.3.3 Impact Testing

Impact testing was performed using a Ceast resil impactor Charpy impact test setup. The hammer was released from an angle of 150$_o$ and hit the sample. The test was performed with a hammer impact energy of 2.75 J and an impact speed of 3.46 m/s. Specimen preparation and testing was conducted according to ISO 179 standard (ISO 179-1, 2010). Each material composition was tested on 5 samples.

3.4. Thermal Tests

3.4.1 Thermal Conductivity

The thermal conductivity tests were performed using a C-Therm Trident instrument. The tests were conducted using the MTPS sensor according to ASTM D7984 (American Society for Testing and Materials, 2021) and the TLS needle sensor according to ASTM D5334 (ASTM D5334, 2014). Thermal conductivity Measurements using the MTPS method were carried out at temperatures ranging from room temperature to 70$_o$C. Three tests were performed on both sides of each specimen. Measurements of thermal conductivity using the TLS method were carried out at a temperature of 175$_o$C. Thermal conductivity of PLA composites reinforced by SFs with various wt% was studied.

3.4.2 Differential Scanning Calorimetry (DSC)

DSC tests were performed using TA Q200 instrument. Degree of crystallinity (X_c) (according to ASTM E794 standard (ASTM E794, 2018)), glass transition temperature (Tg) (according to ASTM E1356 standard (ASTM International, 2008)) and specific heat capacity (C_p) (according to ASTM E1269 standard (ASTM International, 2011)) of the composites were determined. In this experiment, specimens of 5 to10 mg were heated from 0$_o$C to 190$_o$C at a rate of 10$_o$C/min, then waited at 190$_o$C for 5 min to eliminate thermal history, and then reheated to 190$_o$C after cooling to 0$_o$C. In this case, all the thermal parameters were evaluated on the second heating scan and evaluating T_g (glass transition temperature), T_{cc} (cold crystallization temperature), T_m (melting temperature), and X_c (degree of crystallinity) under controlled conditions. X_c was calculated as the ratio between the heat of fusion of the sample ($\Delta H = \Delta H_m - \Delta H_{cc}$, ΔH_m and ΔH_{cc} being the specific melting and cold crystallization enthalpies, respectively), considering only the polymer fraction, and the heat of fusion of 100% crystalline PLA. X_c was determined to analyze the effects of composite process, reinforcements and plasticizers on the crystallinity of PLA. The degree of crystallinity percentage (X_c%) was calculated using the following equation 1.

$$X_c\% = \frac{\Delta Hm - \Delta Hcc}{\Delta H100\% * wPLA} * 100 \qquad (1)$$

where, ΔHm is the measured melting enthalpy, ΔHcc is measured enthalpy of cold crystallization, ΔH100% is melting enthalpy for a theoretical 100% crystalline PLA (93 J/g (Arrigo, Bartoli and Malucelli, 2020)) and wPLA is the weight fraction of PLA. The specific heat capacity (Cp) of neat PLA and PLA based composites as a function of temperature was also obtained using the following equation 2.

$$C_p = \frac{E.\left(\frac{dQ}{dt}\right).60}{\left(\frac{dT}{dt}\right).M} \quad (2)$$

where Cp is specific heat capacity (J/g.oC), E is calibration constant (dimensionless), dQ/dt is heat flow (mW), 60 is conversion constant, dT/dt is heating rate (oC/min) and M is sample mass (mg).

3.4.3 Dynamic Mechanical Analysis (DMA)

DMA is used to measure the mechanical properties of viscoelastic materials as a function of time, temperature and frequency. In this study, three-point bending tests of the specimens as a function of time, temperature and frequency were performed using a Dynamic Mechanical Analyzer (DMA/SDTA 1+ system - Mettler Toledo). The specimen preparation and testing was performed according to ASTM D5023 standard (ASTM D5023-15, 2007). Storage modulus (E'), loss modulus (E'') and the relationship between both moduli (Tan δ) were determined over the range of temperatures from 0oC to 70oC at a frequency of 1.0 Hz. Tan δ is defined as the ratio of loss modulus to storage modulus (E''/E').

3.4.4 Rheology

Rheological testing of composites was performed on melt samples using RheoArt rheometer. In rheological testing using RheoArt rheometer, two capillaries with lengths and diameters of 40 and 2 mm as well as 20 and 1 mm, respectively, at melting temperatures of 190oC and 210oC were used. Experimental tests were carried out to examine the effect of melting temperature and capillary volume on the viscosity of the composites. All samples were dried before testing.

4. RESULTS AND DISCUSSION

4.1. Mechanical Properties

4.1.1 Tensile Properties

Figure 1(a) presents the experimental results that tensile strength of neat PLA was 65.2 MPa, while that of SF-PLA composites decreased to 56.2 MPa and 63.7 MPa with the incorporation of 15 and 20 wt% of SF, respectively. This is due to weak fiber-matrix adhesion strength that leads to stress concentrations within a composite (Tan, Zhang and Qu, 2019). ATBC plasticizer also reduces the tensile strength of the composites. The plasticized PLA shows a 25% decrease compared to neat PLA. For bio-composites, tensile strength drops by 6% at 15 wt% sisal fibers and 17% at 20 wt% compared to their non-plasticized counterparts. This reduction is due to ATBC being weaker than PLA 4043D and its ability to penetrate and weaken PLA molecular chains.

Figure 1(b) also presents that the tensile moduli of SF-PLA composites were 5.4 GPa and 6.2 GPa with 15 and 20 wt% of SF, increased by 58.8% and 82.4%, respectively compared with 3.4 GPa of neat PLA. It is generally accepted that the composite moduli improve with increasing fiber contents. Besides, incorporating ATBC plasticizer reduced stiffness, as plasticizers are less rigid than polymers. Consequently, the elastic modulus decreased by 2% for plasticized PLA, and by 13% and 10% for plasticized composites with 15 wt% and 20 wt% fibers, respectively, compared to their non-plasticized counterparts.

Figure 1(c) also shows that neat PLA showed a tensile strain at break of 4.1%, about 28% higher than the 3.2% of plasticized PLA, likely due to early failure caused by reduced tensile strength from the plasticizer, which weakens intermolecular forces and increases chain mobility. In contrast, non-plasticized SF/PLA composites with 15 wt% and 20 wt% sisal fibers had lower strain at break (3.0% and 2.8%), decreasing by 36.7% and 46.4% relative to neat PLA, due to reduced ductility and load transfer failure at higher fiber content. In addition, plasticizing PLA reduced its tensile strain at failure by 27% compared to neat PLA. Similarly, adding ATBC to composites lowered the strain at failure by 22% (15 wt% SF) and 6% (20 wt% SF) relative to non-plasticized versions. This decrease is due to the fact that the plasticizer can weaken intermolecular forces within the polymer, allowing chains to slide more easily and causing earlier deformation and failure under lower stress (Kassegn, Sirhabizu and Berhanu, 2024).

4.1.2 Flexural Properties

Figure 2(a) illustrates the flexural strength of neat PLA was 81.8 MPa, while the flexural strength of

non-plasticized SF-PLA composites with 15 and 20 wt% of sisal fibers were 94.5 MPa and 101.4 MPa, respectively. This indicates that the content and dispersion of fibers led to efficient load transfer, compensating for the negative effect of poor fiber-matrix interfacial adhesion to a certain extent. On

the other hand, plasticizing PLA reduced its flexural strength by 32% compared to neat PLA. Plasticization lowered flexural strength by 6% at 15 wt% sisal fibers and by 22% at 20 wt% sisal fibers, relative to their non-plasticized counterparts.

Figure 2(b) shows the flexural modulus of SF-PLA composites was 5.2 GPa with SF loading at 20 wt%, increased by 79.3% compared with 2.9 GPa of neat PLA. In addition, plasticized PLA reduced its flexural modulus by 5% compared to neat PLA. The modulus decreased slightly by 0.8% at 20 wt% fibers but increased by 3% at 15 wt% compared to their non-plasticized counterparts.

Figure 2(c) presents that the flexural strain at break of neat PLA was 4.2%, increased by 10.5% compared with 3.8% of plasticized PLA. Flexural strain at break of non-plasticized SF-PLA composites with 15 and 20 wt% of fibers was 2.8%, decreased by 50% compared with 4.2% of neat PLA. This is due to the decrease in ductility of composites with increasing wt% of fibers, leading to load transfer failure. In addition, plasticized PLA reduced its flexural strain at failure by 11% compared to neat PLA. The strain decreased slightly by 4% at 15 wt% SF, but increased by 12% at 20 wt% compared to their non-plasticized counterparts.

4.1.3 Impact Strength

Figure 3 indicates that the impact strength of SF-PLA composites with 20 wt% of sisal fibers was 5.1 kJ/m2, enhanced by 42% compared with 3.6 kJ/m2 of neat PLA. The impact strength of plasticized PLA was 3.8 kJ/m2, increased by 5.6% compared to neat PLA. It can also be seen that the impact strength of plasticized SF-PLA composites with 15 wt% of sisal fibers was 4.7 kJ/m2, improved by 20.5% compared with 3.9 kJ/m2 of non-plasticized SF-PLA composites with 15 wt% of sisal fibers. This indicates ATBC plasticizer enhanced the PLA chain mobility through reducing intermolecular forces between PLA chains, allowing them to be more flexible and increasing their ability to deform under stress. This increased flexibility and mobility help to absorb and distribute the energy generated during impact, reducing the likelihood of brittle failure and enhancing the material's impact resistance.

Moreover, plasticized PLA increased impact strength by 4% compared to neat PLA. For composites, impact strength rose by 22% at 15 wt% fibers but decreased by 6% at 20 wt% compared to the non-plasticized. Overall, impact strength improves with fiber content to an optimum level, then declines. The improvement is attributed to increased chain mobility from the plasticizer, while the limited gain at higher fiber content may be due to fiber effects offsetting the plasticizer's influence.

4.2. Thermal Properties

4.2.1 Thermal conductivity (K)

Figure 4(a) illustrates that the thermal conductivity increases as temperature increases, and then decreases as temperature further increases. In addition, thermal conductivity increases as fiber content in composites increases. Hence, the thermal conductivity of SF-PLA composites with 5 wt% of SF was 0.24 W/mK, raised by 9.1% compared with 0.22 W/mK of neat PLA. It can also be observed that the thermal conductivity of SF-PLA composite with 20 wt% of SF was 0.29 W/mK, raised by 31.8% and 20.8% compared with 0.22 W/mK of neat PLA and SF-PLA composite with 5 wt% of SF, respectively.

Figure 4(b) shows the effect of temperature on the thermal conductivity of a composite. The thermal conductivity of SF-PLA composite containing 20 wt% SF was 0.202 W/m·K at 70°C, representing a 43.6% decrease from 0.29 W/m·K at room temperature. At 175°C, thermal conductivity further decreased to 0.194 W/m·K, corresponding to a 49.5% reduction relative to room temperature. This decline can be attributed to increased molecular chain mobility at elevated temperatures, which reduces thermal conductivity. Additionally, the thermal conductivity at 175°C (0.194 W/m·K) was only 4.1% lower than at 70°C (0.202 W/m·K), indicating a negligible difference within this temperature range. This suggests that temperatures above the glass transition temperature (Tg) have a limited effect on further enhancing polymer chain mobility.

4.2.2 DSC

As shown in Table 2, Tg increased slightly with the addition of SF in PLA without the incorporation of ATBC plasticizer. However, Tg decreased after the incorporation of ATBC plasticizer in PLA regardless of the fiber incorporation. This can be attributed to the increased chain mobility of the SF-PLA composites after the plasticization. In addition, the inclusion of

the fibers and plasticizer increased the crystallinity of the matrix, as also used as nucleating agent.

The SF-PLA composites with the incorporation of ATBC plasticizer failed to cold crystallize in the first heating scan, but crystallized in the second scan, as shown in Figure 5(a). However, SF-PLA composites without the incorporation of the ATBC plasticizer resulted in cold crystallization during the first and second heating scans, as shown in Figure 5(b). This is attributed to the increased crystallization of the PLA matrix with the incorporation of ATBC plasticizer. In contrast, the Tcc of the composites was decreased with the incorporation of ATBC plasticizer, which led to increase the crystallization of PLA matrix.

Figure 6 also presents the specific heat capacity (Cp) of SF-PLA composites was slightly constant before 130oC. However, the Cp of neat PLA was nearly constant before 100oC, and then decreased linearly up to 130oC. A rapid increase in the Cp of SF-PLA composites was observed from 130oC to 150oC, resulting from the change in free volume of PLA. Then Cp quickly decreased up to 160oC, and then it remained constant after 160oC. The Cp of neat PLA was abruptly increased from 130oC to 155oC, and then rapidly declined before 160oC; then it remained constant after 160oC. On the other hand, the Cp increased with the addition of ATBC plasticizer in PLA composites, but the Cp decreased with increasing the wt% of SF in the plasticized composites.

4.2.3 DMA

Figure 7(a) shows a sudden drop in storage moduli of plasticized SF-PLA composites was observed from 45oC to 50oC. However, a drop in the storage modulus of non-plasticized SF-PLA composite was observed from 50oC to 60oC. This decline in storage modulus value from 45oC to 60oC is attributed to the loss of materials' stiffness around Tg. The Tg of plasticized SF-PLA composites declined compared with non-plasticized ones, as shown in Table 2. It is also observed that storage moduli were increased with increasing SF wt%. This trend agrees with the flexural modulus results of SF-PLA composites determined by the Instron testing machine, and is therefore likely to be attributed to increased degree of crystallinity. At room temperature, the plasticized PLA showed a storage modulus of 3.4 GPa, which was raised by 21.4% compared with 2.8 GPa of the same material using the Instron testing machine. With the fiber incorporation, storage moduli increased to 5.0 GPa and 5.4 GPa for SF-PLA composites with 15 wt% and 20 wt% of SF by 47.1% and 58.8%, respectively, compared with 3.4 GPa of plasticized PLA. These storage moduli were slightly increased by 2.0% and 5.9% compared with 4.9 GPa and 5.1 GPa of the same samples tested on the Instron testing machine.

Figure 7(b) illustrates the loss modulus of SF-PLA composites as a function of temperature. It can be observed that the loss modulus peak of plasticized PLA without SF increased significantly after fiber incorporation. Similar to the trend observed in storage modulus curves, the loss modulus peaks of SF-PLA composites with 15 and 20 wt% of SF were higher than plasticized PLA without fiber reinforcement. The increase in the loss modulus peak signifies the increased restrictions in the mobility of the polymer chains due to effective fiber-matrix interaction around Tg. At a temperature above Tg, the loss modulus declined dramatically. This decline in the loss modulus peak can be attributed to an increase in polymer chains' mobility. The increase in mobility of the polymer chains can be due to the fiber attrition and polymer chain scission during processing at a temperature above the Tg. In addition, the loss modulus peaks of the SF-PLA composites with the fiber incorporation were observed to widen compared with PLA without fiber incorporation, leading to the broadening of the glass transition range.

4.2.4 Rheology

Figure 8(a) shows the curves of shear viscosity versus shear rate of PLA composite with the incorporation of 20 wt% of SF and 5 wt% of ATBC plasticizer using RheoArt rheometer. The shear viscosity of the composite was measured with a RheoArt capillary rheometer of 1 mm diameter and 20 mm length at 190oC melt temperature and resulted in a decrease from 1421 Pa.s to 158 Pa.s between shear rates 62 s-1 and 1983 s-1. In addition, the shear viscosity was measured with a capillary rheometer of 2 mm diameter and 40 mm length at 190oC melt temperature and resulted in a decrease from 1275 Pa.s to 172 Pa.s between shear rates 54 s-1 and 1664 s-1. This indicates that the variation in the shear viscosity of the composite material at different diameters and lengths of the capillaries was insignificant. This can be attributed to the uniform fiber distribution in PLA matrix and

effective interactions between fiber-fiber and fiber-matrix. In addition, the shear viscosity was measured with a capillary rheometer of 1 mm diameter and 20 mm length at 210oC melt temperature and resulted in a decrease from 1004 Pa.s to 122 Pa.s between shear rates 52 s-1 and 1606 s-1. This shows that the shear viscosity of the composite declined at 210oC melt temperature compared with the shear viscosity at 190oC melt temperature, for the same diameter and length of the capillary. This is due to the fact that the shear viscosity decreases as the melt temperature increases.

Figure 8(b) presents that the shear viscosity of SF-PLA composite with 20 wt% of SF at lower shear rate was 1508 Pa.s, increased by 18.1% and 7.1% compared with 1277 Pa.s of neat PLA and 1408 Pa.s of the composite with 10 wt% of SF, respectively. The increased shear viscosity of SF-PLA composites reflects the effects of strong fiber-fiber interactions and interactions with PLA chains because of short length and good distribution of the fiber. This can be explained by the fact that the interactions of fiber-fiber and fiber with polymer limits the PLA chain mobility, especially at increased fiber wt%. In this regard, the shear viscosity of SF-PLA composites increasing with increasing SF wt%. In contrast, the variation in shear viscosity of the composites wasn't significant at higher range of shear rates. The shear viscosity of the composites with 20 wt% of SF and 10 wt% of SF were 43 Pa.s at a shear rate of 11714 s-1 and 44 Pa.s at a shear rate of 9842 s-1, respectively. The shear viscosity of neat PLA was 50 Pa.s at a shear rate of 8971 s-1. The viscosity curves overlapping each other at higher shear rate can be attributed to the insignificant effect of fillers, leads to an increase in chain mobility as shear rate increases.

Figure 8(c) depict the measured pressures required for each capillary length. The results demonstrate that negative values were not observed when utilizing the trend line, as this can be attributed to the accuracy of the gap, loading, and material properties. Moreover, the findings indicate that the diameter of the capillaries did not exert a notable influence on the viscosity of the sisal fiber reinforced PLA composite material. On the other hand, when employing the long capillary, the pressure was doubled, and additional heating was applied at the bottom of the capillary.

5. CONCLUSION

The findings of this study show that the incorporation of short SF into PLA significantly enhances stiffness and impact performance, as reflected by increased tensile and flexural moduli and improved impact strength, despite a reduction in tensile strength at lower fiber content. The addition of ATBC plasticizer adversely affects tensile and flexural properties while further enhancing impact strength. Thermal analysis shows that thermal conductivity increases with both SF and ATBC but decreases with rising temperature. DSC results confirm that ATBC promote crystallinity, with ATBC acting as a nucleating agent by increasing crystallinity and reducing glass transition and crystallization temperatures. Specific heat capacity increases with ATBC but declines with fiber loading. DMA results are consistent with flexural properties, highlighting strong dependence on fiber content and temperature, particularly near the glass transition region.

Acknowledgements

The author would like to appreciate the members of the research group Propolis at KU Leuven Bruges campus for their support while specimen preparation and performing experimental tests. Secondly, the author want to thank all the KU Leuven community for their contribution in one or another way while doing the research work.

Funding: No funding

Data Availability Statement: The data used to support the findings of this study are available from the author upon reasonable request.

Declarations: The author declares no known conflicts of interest with respect to the research, authorship and publication of this article.

REFERENCES

Akderya, T., Özmen, U. and Baba, B. O. (2020) 'Investigation of long-term ageing effect on the thermal properties of chicken feather fibre/poly(lactic acid) biocomposites', Journal of Polymer Research, 27(6). doi: 10.1007/s10965-020-02132-2.

Ali, A. et al. (2018) 'Hydrophobic treatment of natural fibers and their composites—A review', Journal of Industrial Textiles, 47(8), pp. 2153–2183. doi: 10.1177/1528083716654468.

American Society for Testing and Materials (2021)

'Standard Test Method for Measurement of Thermal Effusivity of Fabrics Using a Modified Transient Plane Source (MTPS) Instrument, ASTM D7984', ASTM International Standards, i, pp. 1–5. doi: 10.1520/D7984-16.2.

Arrigo, R., Bartoli, M. and and Malucelli, G. (2020) 'polymers Poly (lactic Acid)– Biochar Biocomposites : E ff ect of Processing and Filler Content on Rheological ', pp. 1–13.

ASTM D5023-15 (2007) 'Standard Test Method for Plastics: Dynamic Mechanical Properties: In Flexure (Three-Point Bending)', ASTM International, 08, pp. 9–12.

ASTM D5334 (2014) 'Astm D5334', Annual Book of ASTM Standards, (Agosto), pp. 1–8. doi: 10.1520/D5334-0814.2.

ASTM E794 (2018) 'Standard Test Method for Melting And Crystallization Temperatures By Thermal Analysis', Ast, 06(Reapproved), p. 4.

ASTM International (2008) 'Standard Test Method for Assignment of the Glass Transition Temperatures by Differential Scanning Calorimetry', ASTM International, 08(E1356), pp. 1–4. doi: 10.1520/E1356-08R14.2.

ASTM International (2011) 'E1269-11 : Standard Test Method for Determining Specific Heat Capacity by Differential Scanning Calorimetry', Astm, 14, p. 6. doi: 10.1520/E1269-11.2.

Backes, E. H. et al. (2019) 'Analysis of the degradation during melt processing of pla/biosilicate® composites', Journal of Composites Science, 3(2). doi: 10.3390/jcs3020052.

Bekele, A. E., Lemu, H. G. and Jiru, M. G. (2022) 'Experimental study of physical, chemical and mechanical properties of enset and sisal fibers', Polymer Testing, 106(August 2021), p. 107453. doi: 10.1016/j.polymertesting.2021.107453.

Cataldi, P. et al. (2020) 'Multifunctional Biocomposites Based on Polyhydroxyalkanoate and Graphene / Carbon Nano fi ber Hybrids for Electrical and Thermal Applications'. doi: 10.1021/acsapm.0c00539.

Cheour, K. et al. (2020) 'Long-term Immersion in Water of Flax-glass Fibre Hybrid Composites : Effect of Stacking Sequence on the Mechanical and Damping Properties', 21(1), pp. 162–169. doi: 10.1007/s12221-020-9494-7.

Choudhury, M. R. and Debnath, K. (2019) 'Experimental analysis of tensile and compressive failure load in single-lap bolted joint of green composites', Composite Structures, 225(April), p. 111180. doi: 10.1016/j.compstruct.2019.111180.

Cristina, K. et al. (2020) 'Thermal characterization and lifetime prediction of the PHBV / nanocellulose biocomposites using different kinetic approaches', 0123456789, pp. 7503–7522. doi: 10.1007/s10570-020-03318-z.

Delgado-Aguilar, M. et al. (2017) 'Bio composite from bleached pine fibers reinforced polylactic acid as a replacement of glass fiber reinforced polypropylene, macro and micro-mechanics of the Young's modulus', Composites Part B: Engineering, 125, pp. 203–210. doi: 10.1016/j.compositesb.2017.05.058.

Depuydt, D. et al. (2017) 'Digital image correlation as a strain measurement technique for fibre tensile tests', Composites Part A: Applied Science and Manufacturing, 99, pp. 76–83. doi: 10.1016/j.compositesa.2017.03.035.

Dwivedi, S., Pattnaik, S. and Kumar Sutar, M. (2021) 'Tensile properties and regression analysis of natural fiber and intralaminar mat reinforcement', Materials Today: Proceedings, (xxxx). doi: 10.1016/j.matpr.2020.11.963.

Elsawy, M. A. et al. (2017) 'Hydrolytic degradation of polylactic acid (PLA) and its composites', Renewable and Sustainable Energy Reviews, 79(May), pp. 1346–1352. doi: 10.1016/j.rser.2017.05.143.

Gupta, M. K. and Singh, R. (2018) 'Flexural and Dynamic Mechanical Analysis (DMA) of Polylactic Acid (PLA) Coated Sisal Fibre Reinforced Polyester Composite', Materials Today: Proceedings, 5(2), pp. 6109–6114. doi: 10.1016/j.matpr.2017.12.216.

Haque, R. et al. (2015) 'Fibre-matrix adhesion and properties evaluation of sisal polymer composite', Fibers and Polymers, 16(1), pp. 146–152. doi: 10.1007/s12221-015-0146-2.

ISO (2006) 'ISO 527-1:2019. Plastics—Determination of Tensile Properties—Part 1: General Principles', 527-1, 2012(527–1), p. 13.

ISO (2019) 'INTERNATIONAL STANDARD Plastics — Determination of flexural properties', Iso 178, 2019.

ISO 179-1 (2010) 'Plastics - Determination of Charpy impact properties', ISO - International Standards Organization, (1110), pp. 1–11.

Jing, H. et al. (2021) 'Study on properties of polylactic acid/lemongrass fiber biocomposites prepared by fused deposition modeling', Polymer Composites, 42(2), pp. 973–986. doi: 10.1002/pc.25879.

Kassegn, E. et al. (2021) Study on Effects of Process Parameters on Mechanical Behaviors of Injection Molded Glass Fiber Reinforced Polypropylene Matrix Composite, Lecture Notes of the Institute for Computer Sciences, Social-Informatics and

Telecommunications Engineering, LNICST. Springer International Publishing. doi: 10.1007/978-3-030-80618-7_32.

Kassegn, E. et al. (2023) 'Investigating the Dimensional , Mechanical , and Morphological Properties of Composites Reinforced with Sisal Fibers and Polylactic Acid in Response to Water Absorption', 2023.

Kassegn, E., Sirhabizu, B. and Berhanu, T. (2024) 'A study of the mechanical , thermal and rheological properties of sisal fi ber-reinforced polylactic acid bio-composites with tributyl 2-acetylcitrate as a plasticizer', 0(0), pp. 1–24. doi: 10.1177/08927057241235649.

Khan, A. Z. (2019) 'Effect of plasticizer on physical and mechanical properties of ldpe / sago starch blend Effect of plasticizer on physical and mechanical properties of ldpe / sago starch blend'. doi: 10.1088/1742-6596/1150/1/012032.

Lalit, R., Mayank, P. and Ankur, K. (2018) 'Natural fibers and biopolymers characterization: A future potential composite material', Strojnicky Casopis, 68(1), pp. 33–50. doi: 10.2478/scjme-2018-0004.

Liu, T. et al. (2021) 'Damping behavior of plant fi ber composites : A review', Composite Structures, 275(June), p. 114392. doi: 10.1016/j.compstruct.2021.114392.

Mann, G. S. et al. (2020) 'Green composites: A review of processing technologies and recent applications', Journal of Thermoplastic Composite Materials, 33(8), pp. 1145–1171. doi: 10.1177/0892705718816354.

Morales, A. P. et al. (2017) 'Bamboo-polylactic acid (PLA) composite material for structural applications', Materials, 10(11), pp. 1–22. doi: 10.3390/ma10111286.

Murariu, M. and Dubois, P. (2016) 'PLA composites: From production to properties', Advanced Drug Delivery Reviews, 107, pp. 17–46. doi: 10.1016/j.addr.2016.04.003.

Ortenzi, M. A. et al. (2020) 'Synthesis of polylactic acid initiated through biobased antioxidants: Towards intrinsically active food packaging', Polymers, 12(5). doi: 10.3390/POLYM12051183.

Qi, X., Ren, Y. and Wang, X. (2017) 'New advances in the biodegradation of Poly(lactic) acid', International Biodeterioration and Biodegradation, 117, pp. 215–223. doi: 10.1016/j.ibiod.2017.01.010.

Saeed, U., Nawaz, M. A. and Al-Turaif, H. A. (2018) 'Wood flour reinforced biodegradable PBS/PLA composites', Journal of Composite Materials, 52(19), pp. 2641–2650. doi: 10.1177/0021998317752227.

Sanjay, M. R. et al. (2018) 'Characterization and properties of natural fiber polymer composites: A comprehensive review', Journal of Cleaner Production, 172, pp. 566–581. doi: 10.1016/j.jclepro.2017.10.101.

Sanjay, M. R. and Yogesha, B. (2018) 'Studies on hybridization effect of jute/kenaf/E-glass woven fabric epoxy composites for potential applications: Effect of laminate stacking sequences', Journal of Industrial Textiles, 47(7), pp. 1830–1848. doi: 10.1177/1528083717710713.

Selvaraj, D. K. et al. (2019) 'Influence of the natural additive on natural fiber reinforced thermoplastic composite', Procedia Manufacturing, 38(2019), pp. 1121–1129. doi: 10.1016/j.promfg.2020.01.200.

Snowdon, M. R. et al. (2019) 'Comparative study of the extrinsic properties of poly(lactic acid)-based biocomposites filled with talc: Versus sustainable biocarbon', RSC Advances, 9(12), pp. 6752–6761. doi: 10.1039/c9ra00034h.

Tan, Y., Zhang, X. and Qu, J. P. (2019) 'Preparation and characterization of poly(lactic acid)/sisal fiber bio-composites under continuous elongation flow', Journal of Polymer Engineering, 39(1), pp. 76–84. doi: 10.1515/polyeng-2018-0075.

Veerasimman, A. et al. (2022) 'Thermal Properties of Natural Fiber Sisal Based Hybrid Composites–A Brief Review', Journal of Natural Fibers, 19(12), pp. 4696–4706. doi: 10.1080/15440478.2020.1870619.

Zhang, J. et al. (2020) 'High-performance lignocellulose / polycarbonate biocomposites fabricated by in situ reaction : Structure and properties', Composites Part A, 138(August), p. 106068. doi: 10.1016/j.compositesa.2020.106068.